Low-Energy (<10 meV) Feature in the Nodal Electron Self-Energy and Strong Temperature Dependence of the Fermi Velocity in $Bi_2Sr_2CaCu_2O_{8+\delta}$

N. C. Plumb,[1,*] T. J. Reber,[1] J. D. Koralek,[2] Z. Sun,[1] J. F. Douglas,[1] Y. Aiura,[3] K. Oka,[3] H. Eisaki,[3] and D. S. Dessau[1,4,†]

[1]*Department of Physics, University of Colorado, Boulder, Colorado 80309-0390, USA*

[2]*Materials Science Division, Lawrence Berkeley National Laboratory, Berkeley, California 94720, USA*

[3]*AIST Tsukuba Central 2, 1-1-1 Umezono, Tsukuba, Ibaraki 305-8568, Japan*

[4]*JILA, University of Colorado and NIST, Boulder, Colorado 80309-0440, USA*

(Received 27 April 2010; published 22 July 2010)

Using low photon energy angle-resolved photoemission, we study the low-energy dispersion along the nodal (π, π) direction in $Bi_2Sr_2CaCu_2O_{8+\delta}$ as a function of temperature. Less than 10 meV below the Fermi energy, the high-resolution data reveal a novel ''kinklike'' feature in the electron self-energy that is distinct from the larger well-known kink roughly 70 meV below E_F. This new kink is strongest below the superconducting critical temperature and weakens substantially at higher temperatures. A corollary of this finding is that the Fermi velocity v_F, as measured in this low-energy range, varies rapidly with temperature—increasing by almost 30% from 70 to 110 K. The behavior of $v_F(T)$ appears to shift as a function of doping, suggesting a departure from simple ''universality'' in the nodal Fermi velocity of cuprates.

DOI: 10.1103/PhysRevLett.105.046402 PACS numbers: 71.18.+y, 74.25.Jb, 74.72.−h, 79.60.−i

Angle-resolved photoemission spectroscopy (ARPES) is a direct and powerful probe of electrons and their interactions in solids and an ideal tool for studying complex materials. Recently, ARPES has accessed a low-energy photon regime that has substantially improved the technique's resolution, paving the way for several new discoveries [1–4]. In this Letter we employ low-energy photons to reveal a new interaction effect in $Bi_2Sr_2CaCu_2O_{8+\delta}$ (Bi2212)—this one located less than 10 meV below E_F. This feature, occurring in the electron self-energy Σ along the nodal (gapless) direction of the Fermi surface (FS), has a rapid onset as T drops below the superconducting critical temperature T_c. Correspondingly, v_F has a similar strong T dependence. While electron scattering rate measurements from ARPES have hinted at the existence of this renormalization [4], this is its first convincing and detailed observation.

High energy resolution has proved crucial to the identification of this new self-energy feature. As we will show, energy broadening effects strongly impede attempts to reliably obtain band dispersions near E_F at low T. The energy broadening is the combination of the analyzer resolution, photon bandwidth, photoelectron final state lifetimes, and inelastic scattering. All these broadening mechanisms are minimized by shifting from conventional ARPES photon energies ($h\nu \sim 20$–100 eV) to low energies ($h\nu \sim 6$–7 eV). Low-$h\nu$ light sources themselves generally have ultrahigh energy resolution, typically reducing the combined resolution of the photons and analyzer to just a few meV. Additionally, extrinsic spectral broadening due to the photoelectrons' final state lifetimes [1] is reduced, and their mean free paths are increased by a factor of 3–10, thereby minimizing inelastic scattering and increasing bulk sensitivity. Moreover, low photon energy yields superb momentum resolution compared to conventional ARPES. As a result, laser and low-energy ARPES have observed the sharpest spectra from the cuprates to date, representing the best attempts so far at obtaining the intrinsic spectral functions of these materials [1,3]. While resolution is significantly improved for $h\nu = 6$–7 eV, the overall dispersions obtained agree closely with conventional data down to at least $\sim$150 meV below E_F, signaling there is no obvious breakdown in the sudden approximation for these states. This is especially true for the near-E_F energy scale that is the focus of this Letter, as these states are the longest-lived.

In this work, single crystals of Bi2212 were studied using the laser ARPES system at the University of Colorado [5] with $h\nu = 6$–7 eV, as well as beam line 5-4 at the Stanford Synchrotron Radiation Laboratory (SSRL) with $h\nu = 7$ eV. For the data shown here, $h\nu = 7$ eV and the total energy resolution ΔE (photon bandwidth and analyzer resolution) was about 4–5 meV FWHM. Samples were prepared as originally described in [1]. For optimally doped (OP) samples, $T_c = 91$–92 K, while the overdoped (OD) sample studied had $T_c \approx 62$ K. Some minor response nonlinearity of the detectors used in ARPES is known to exist [6], but has been checked to not affect the key findings presented here. The analysis process for measuring the band dispersion is illustrated in Fig. 1. As has become the standard recently, we utilize momentum distribution curves (MDCs)—cuts through the ARPES spectrum at constant energies [7]. The Lorentzian peak locations at each energy are taken to mark the dispersion.

Studies of the fine details of the low-energy nodal spectra require unusual alignment accuracy, because the presence of even a small gap just off the node can have a

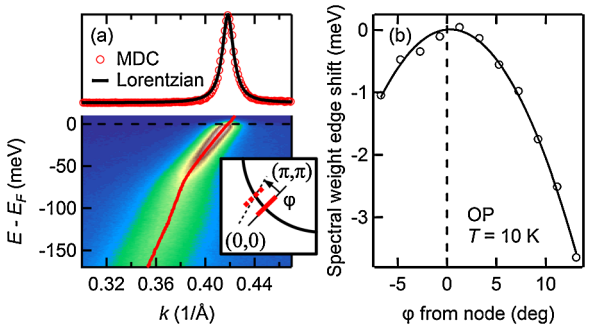

FIG. 1 (color online). Raw ARPES data (a). The horizontal dashed line is a single MDC, shown above, which is fit with a Lorentzian. The Lorentzian peak positions at each energy mark the band dispersion [solid gray (red) line]. The inset is a schematic of the ARPES cut [gray (red) line] along the nodal (π, π) direction in the first quadrant of the Brillouin zone. Nodal alignment is verified by scanning the ARPES cut to study the FS geometry, band velocity, and leading edge of the spectral weight (an indicator of the gap). As an example, the spectral weight edge (b) agrees with the node as determined by FS geometry (0°) to better than 1° along ϕ.

significant effect on the near-E_F dispersion. In addition to the usual Laue diffraction method for azimuthal sample orientation, we took special care to spectroscopically ensure that the dispersions studied were as close to nodal as possible. By scanning perpendicular to the ARPES cut, we examined the FS geometry, band velocities, and superconducting gap near the node as a function of the azimuthal angle ϕ [inset of Fig. 1(a)]. For example, Fig. 1(b) shows the relative shift in energy of the spectral weight edge [8] (an indirect measure of the gap) as a function of ϕ. The maximal gapping of the "nodal" spectra is under 1 meV and insignificant compared to the scale of the new self-energy effects reported in this work (located ~5–10 meV below E_F).

Typically, MDC fitting results are taken at face value. While this is acceptable for most energies, in the vicinity of an energetically sharp shift in spectral weight (e.g., near E_F), MDC analysis will not yield fully accurate dispersion data if ΔE is greater than or comparable to the width of the spectral transition [9]. For the fine-scale data near E_F discussed here, this is an automatic concern and highlights the clear benefit of ultrahigh-resolution low-$h\nu$ ARPES. With that said, for simplicity's sake, we will first demonstrate the existence and behavior of the new self-energy feature (nominally the "10-meV" kink) using only raw data. Later on we will turn to the more complicated task of considering the role of ΔE. The analysis will show that when such effects are taken into account, the case for the 10-meV kink is even more robust, with v_F varying dramatically and essentially monotonically over the full temperature range studied.

Figure 2(a) illustrates the temperature behavior of the nodal dispersion. To extract Σ, the "bare" noninteracting dispersion must be known. Presently there is no agreed-upon method to obtain the bare band from the data. Our approach is to assume a linear band connecting two points on the measured dispersion that do not change significantly as a function of T. This choice of dispersion is at least noninteracting with respect to certain T-dependent phenomena. We employ this bare band to assess key features of ReΣ, as seen in Figs. 2(b) and 2(c). The most prominent aspect of the self-energy data presented here is, of course, the well-known "70-meV" kink [10] in ReΣ [Fig. 2(b)] and corresponding rise in ImΣ [Fig. 2(c)]. In addition to the 70-meV kink, however, a novel bend or kinklike feature is visible at low T, located less than 10 meV below E_F [arrow in Fig. 2(b)]. This feature is especially evident in the change in ReΣ from 130 to 70 K [upper portion of Fig. 2(b)]. Likewise, ImΣ displays a subtle T-dependent feature within roughly 10 meV of E_F, illustrated by the decrease in ImΣ from 130 to 10 K at this energy scale [arrow in Fig. 2(c)]. These findings qualitatively agree with the observations of [4], though they were not discussed in their text, except for one mention of a "possible feature" in the MDC widths.

As mentioned previously, at low T and very near E_F, energy broadening causes the MDC peaks of a dispersive band to deflect to lower momenta k [9]—the *opposite*

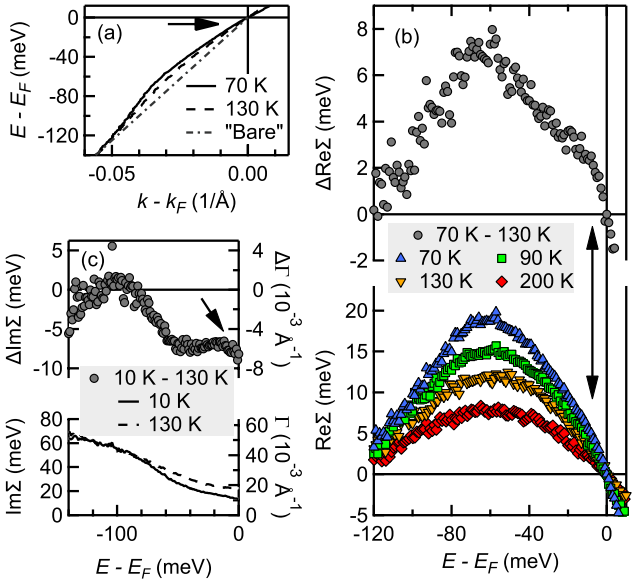

FIG. 2 (color online). MDC-derived dispersions from raw data from nodal Bi2212 (a). The "bare band" (dash-dotted line) is assumed in order to extract ReΣ, shown in the lower portion of (b). Besides the well-known peak at about 70 meV, there is a low-energy (<10 meV) feature in ReΣ occurring below T_c [black arrows in (a) and (b)]. The low-energy feature is especially evident in the change in ReΣ from 130 to 70 K [upper portion of (b)]. At the same energy scale there is also a subtle feature in ImΣ at sufficiently low T [lower portion of (c)], as illustrated by looking at the change in ImΣ from 130 to 10 K [upper portion of (c)].

direction of the observed kink. Hence ΔE weakens the appearance of this feature at low T. The effect is illustrated in Figs. 3(a) and 3(b). Ungapped ARPES spectra were simulated with a linear dispersion through E_F using realistic parameters for nodal data [11] and then convolved with Gaussian resolution functions. Lorentzian fits to the resulting simulated MDCs were then performed in the standard way. The MDC peak deflection seen in the simulations causes the measured Fermi velocity to be greater than the true v_F. The effect becomes more significant as either T is decreased or ΔE is increased. Note that k resolution does not have an effect on MDC fitting, since there is no sharp transition in spectral weight along the k axis for a MDC [although there is one for the *energy-integrated* spectrum $n(k)$].

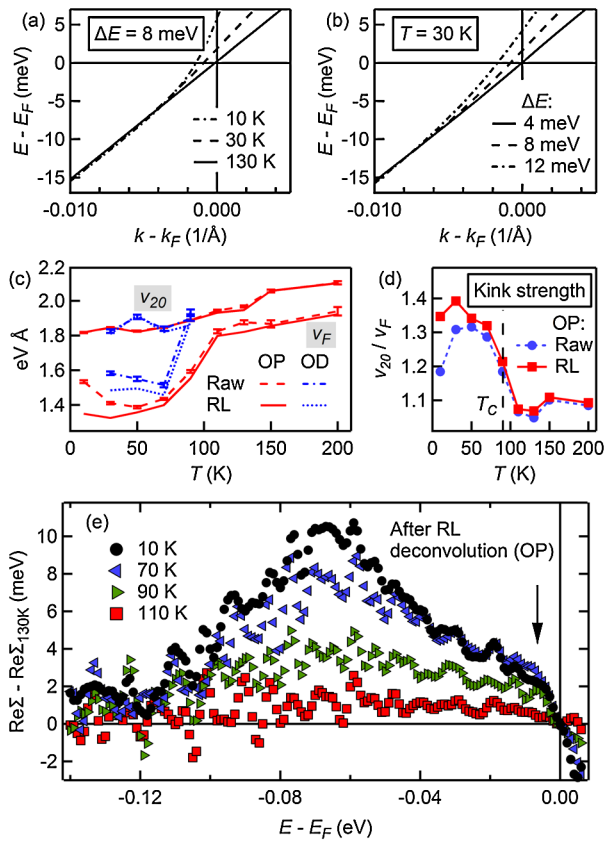

FIG. 3 (color online). Simulated ARPES spectra show how near-E_F MDC dispersions deflect to lower momenta as either (a) T is decreased or (b) ΔE is increased. Hence the raw v_F's in (c) have an artificial upturn below $\sim$50 K. The upturn effectively can be removed using 2D RL deconvolution, revealing essentially monotonic $v_F(T)$ while the deeper v_{20} is unaffected. Optimal (OP) and overdoped (OD) v_F and v_{20} show similar behavior, except that the shift in v_F occurs at a lower T for OD (roughly shifting with T_c). (d) "Kink strength" ($\equiv v_{20}/v_F$) increases sharply near T_c. (e) The near-T_c onset of the 10-meV kink (arrow) is seen in the change in ReΣ relative to 130 K.

To better study the true, underlying behavior of $v_F(T)$, we have removed the effects of ΔE by performing a 2D Richardson-Lucy (RL) deconvolution [12]. The technique successfully corrects the dispersion, though at the expense of adding some small ripple. It has been validated by simulations such as those in Figs. 3(a) and 3(b), which agree well with the results of the deconvolution.

To illustrate the dispersion behavior above and below the 10-meV kink, we define a band velocity v_{20} in addition to v_F. Whereas v_F is obtained by a linear fit to the dispersion over the range $E_F \pm 5$ meV, v_{20} is computed by fitting from 30 to 10 meV below E_F. The velocities found from the deconvolved spectra are shown in Fig. 3(c). Deconvolution has little effect on the observed v_F for $T \gtrsim 50$ K and a negligible effect on v_{20} at all temperatures. For $T \lesssim 50$ K, however, the RL results show no significant upturn in v_F, making $v_F(T)$ essentially monotonic while preserving the dramatic change in v_F relative to v_{20} near T_c. The low-energy "kink strength," defined as the ratio v_{20}/v_F, increases sharply below $\sim$100 K and possibly saturates below $\sim$70 K [Fig. 3(d)]. This behavior is evident in ReΣ of the deconvolved spectra. Figure 3(e) shows the change in ReΣ from its value at 130 K. Here again the new low-energy feature (arrow) rises quickly as T drops through 90 K and appears to level off at lower temperatures. The main 70-meV peak, however, continues to grow as T is lowered down to 10 K.

The new results here have implications for the concept of a "universal" nodal v_F in the cuprates [13]. Based on a somewhat qualitative comparison of dispersions at an energy scale comparable to what we have defined for v_{20}, the authors of [13] concluded that "v_F" is nearly independent of doping. Figure 3(c) compares OP band velocities to those of an OD sample ($T_c \approx 62$ K). Although v_{20} varies with T, it is not substantially affected by doping. This agrees with [13] to the extent that they did not distinguish between the v_F and v_{20} energy scales. Unlike v_{20}, however, the behavior of v_F does depend on doping. While $v_F(T)$ follows the same general trend for OD and OP, the steep portions of the two curves (i.e., the 10-meV kink "onsets") do not overlap. This is an interesting finding that merits further study. It implies that the concept of a universal nodal v_F is only relevant over a limited energy range deeper than the 10-meV kink.

The origin of the 10-meV kink should be of great interest, because its T dependence suggests that it may be associated with high-temperature superconductivity. As has been proposed for the 70-meV kink, the 10-meV kink could arise from coupling to a bosonic mode (e.g., a phonon) or, as will be discussed, other possibilities may exist as well.

Theoretical calculations have routinely predicted a sizable, distinct peak in the phonon density of states near or below 10 meV in cuprates [14]. Moreover, various experiments have observed phonons at this energy scale [15].

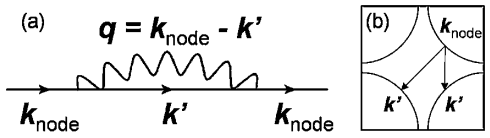

FIG. 4. (a) Feynman diagram of a nodal electron-phonon interaction in the Migdal-Eliashberg approach. Below T_c, an electron at k_{node} is scattered to k' by a phonon with energy Ω and momentum transfer $q = k_{\mathrm{node}} - k'$. The corresponding self-energy feature observed by ARPES will appear at $\omega = -(\Omega + \Delta_{k'})$. (b) Fermi surface with examples of q scattering vectors for bosonic coupling such that $\Delta_{k'} \approx 0$.

However, a generic feature of electron-boson coupling theories is that self-energy features observed by ARPES should be shifted by the d-wave gap energy $\Delta_{k'}$ of the relevant k' states to which the nodal electrons couple [16] [Fig. 4(a)]. This constrains any explanation of the 10-meV kink in terms of bosonic coupling, because the gap maximum $\Delta_{\mathrm{max}} \approx 35$ meV at the antinode is a larger energy scale than the kink itself. Hence, if bosonic coupling is responsible for the 10-meV kink, the scattering must be confined to near-nodal (small gap) states [Fig. 4(b)].

In an alternative to the electron-boson coupling paradigm, Chubukov and Eremin have recently claimed that the observed T scaling of v_F is consistent with corrections to Fermi liquid (FL) theory in 2D and that the form and size of the low-energy feature are roughly what is expected [17]. The correction ultimately arises from the nonanalytic $\mathrm{Im}\Sigma \sim \omega^2 \ln\omega$ term due to $2k_F$ backscattering in a 2D FL, hence connecting the ungapped portions of the FS and avoiding theoretical complications related to the gap.

A low-energy crossover in the electronic scattering rate, such as predicted by marginal Fermi liquid (MFL) behavior [18], potentially could be relevant. However, MFL theory is characterized by $\mathrm{Im}\Sigma \propto \max(|\omega|, k_B T)$, presumably with some smooth crossover behavior at $|\omega| = k_B T$. Hence the theory predicts the kink location should vary with T, which is so far not apparent in the data.

In conclusion, a new kinklike electron self-energy feature has been observed along the superconducting node in Bi2212 less than 10 meV below E_F. It is visible for $T \lesssim T_c$ and weakens rapidly at higher T. Associated with this feature, v_F scales substantially—increasing by roughly 30% from 70 to 110 K. The overall behavior of $v_F(T)$ appears to shift with doping, which conflicts with the supposed universal nodal v_F in cuprates. The T dependence of the feature suggests a possible role in high-temperature superconductivity, although it is unclear at this time what mechanism(s) may lead to this low-energy renormalization.

Funding was provided by DOE Grant No. DE-FG02-03ER46066 with partial support from the NSF EUV ERC and KAKENHI (19340105). We thank A. V. Chubukov, T. P. Devereaux, S. Johnston, and K. Shimada for valuable conversations. Q. Wang, J. Griffith, S. Cundiff, H. Kapteyn, and M. Murnane lent assistance. D. H. Lu and R. G. Moore assisted at SSRL. SSRL is operated by the DOE, Office of Basic Energy Sciences.

Note added.—During the review process following the submission of this Letter, related works showing the low-energy kink appeared [19].

*plumbnc@colorado.edu
†dessau@colorado.edu

[1] J. D. Koralek *et al.*, Phys. Rev. Lett. **96**, 017005 (2006).
[2] T. Yamasaki *et al.*, Phys. Rev. B **75**, 140513 (2007); H. Iwasawa *et al.*, Phys. Rev. Lett. **101**, 157005 (2008); K. Ishizaka *et al.*, Phys. Rev. B **77**, 064522 (2008).
[3] P. A. Casey *et al.*, Nature Phys. **4**, 210 (2008).
[4] W. Zhang *et al.*, Phys. Rev. Lett. **100**, 107002 (2008).
[5] J. D. Koralek *et al.*, Rev. Sci. Instrum. **78**, 053905 (2007).
[6] N. Mannella *et al.*, J. Electron Spectrosc. Relat. Phenom. **141**, 45 (2004); T. J. Reber *et al.* (unpublished).
[7] T. Valla *et al.*, Science **285**, 2110 (1999).
[8] The spectral weight edge is determined by fitting a Fermi function to a plot of the area under each MDC Lorentzian as a function of energy. After precisely finding the node at $T = 10$ K, the energy scales of subsequent higher-T spectra were adjusted according to their spectral weight edges in order to correct for any minor inconsistencies, such as small drifts in the photon energy.
[9] N. J. C. Ingle *et al.*, Phys. Rev. B **72**, 205114 (2005).
[10] P. V. Bogdanov *et al.*, Phys. Rev. Lett. **85**, 2581 (2000); A. Lanzara *et al.*, Nature (London) **412**, 510 (2001); P. D. Johnson *et al.*, Phys. Rev. Lett. **87**, 177007 (2001); A. Kaminski *et al.*, *ibid.* **86**, 1070 (2001); A. D. Gromko *et al.*, Phys. Rev. B **68**, 174520 (2003).
[11] The simulations shown use a linear dispersion and a quadratic scattering rate that is roughly consistent with the experimental data. The findings are not sensitive to the form of the scattering rate (e.g., linear or quadratic).
[12] W. H. Richardson, J. Opt. Soc. Am. **62**, 55 (1972); L. B. Lucy, Astron. J. **79**, 745 (1974); H.-B. Yang *et al.*, Nature (London) **456**, 77 (2008).
[13] X. J. Zhou *et al.*, Nature (London) **423**, 398 (2003).
[14] W. Kress *et al.*, Phys. Rev. B **38**, 2906 (1988); M. G. Stachiotti *et al.*, Physica (Amsterdam) **243C**, 207 (1995); F. Giustino, M. L. Cohen, and S. G. Louie, Nature (London) **452**, 975 (2008).
[15] A. A. Tsvetkov *et al.*, Phys. Rev. B **60**, 13 196 (1999); M. d'Astuto *et al.*, J. Phys. Condens. Matter **15**, 8827 (2003); A. Gauzzi *et al.*, Phys. Rev. B **75**, 144511 (2007).
[16] T. P. Devereaux *et al.*, Phys. Rev. Lett. **93**, 117004 (2004).
[17] A. Chubukov and I. Eremin, Phys. Rev. B **78**, 060509 (2008).
[18] C. M. Varma *et al.*, Phys. Rev. Lett. **63**, 1996 (1989).
[19] J. D. Rameau *et al.*, Phys. Rev. B **80**, 184513 (2009); I. M. Vishik *et al.*, Phys. Rev. Lett. **104**, 207002 (2010); H. Anzai *et al.*, arXiv:1004.3961.